CALIBRATION AND RESOLUTION WITH CURRENT CLEO FIELD

R. HOLMES

1. Introduction

The calibration work reported previously[1][2] was done using simulations incorporating an earlier (and now unknown) version of the CLEO solenoid field. The functional form I developed to extract momentum from two hit positions does not work with the current CLEO field. A somewhat messier version seems to be required, especially after fixing a problem that caused chaotic trajectory fluctuations. Momenta and angles, hence Q^2, can be determined accurately from hit pairs even for a field that deviates significantly from the model, and resolutions can be determined.

2. Recap

In the preceding work I used the following variables (I have changed notation a bit here):

The cylindrical coordinates of the vertex are (r_v, ϕ_v, z_v); in the following we take $r_v = 0$. The momentum of the scattered electron is parameterized by magnitude p, polar angle θ_p, and azimuthal angle ϕ_p (all taken to be in the lab frame). For this work $1/p$ is generally better to work with than p. Hit coordinates in chamber i (i=1..5) are (r_i, ϕ_i, z_i) in cylindrical coordinates.

By symmetry, the quantities $\Delta\phi_{ij} \equiv \phi_i - \phi_j$, $\Delta r_{ij} \equiv r_i - r_j$, and $\langle r\rangle = \frac{1}{2}(r_i + r_j)$ are independent of ϕ_p and dependent on p, θ_p, and z_v. $\Delta z_{ij} \equiv z_i - z_j$ and $\langle z_{ij}\rangle \equiv \frac{1}{2}(z_i - z_j)$ are constants for any pair of detectors. The double subscripts will often be suppressed here, and for convenience in comparing one pair of GEMs to another, I normalize $\Delta\phi$ and Δr by Δz, and $\langle r\rangle$ by $\langle z\rangle$. For a uniform field one expects $1/(p\Delta\phi)$ to be a function of Δr and constant with respect to $1/p$, $\Delta\phi$, and $\langle r\rangle$. I found that for the version of the CLEO field I was using then, $1/(p\Delta\phi)$ was still constant with respect to $1/p$ and $\Delta\phi$, though the functional form of its dependence on Δr was different from the uniform field case and the functional parameters depended on $R \equiv \Delta r/\langle r\rangle$. A cubic in Δr whose polynomial coefficients were linear functions of R gave good fits.

3. Simulations

For the first part of the work reported here I used simulations containing only the magnetic field and non-material virtual detectors at the positions of the GEMs; no components made of non vacuum materials are present. I used truth values of the hit positions, with no resolution smearing. Except as indicated I used the "solenoid_CLEOv8" field and the version of the GEMC 2 and solid_gemc software in the repositories as of August 2015. The

two data sets are simulated elastics with beam energies 4.4 and 6.6 GeV, and what I call "uniform": electrons distributed uniformly in $p > 2$ GeV/c, θ_p, ϕ_p, and z_v, with cuts then applied to select electrons within the kinematic range of interest: $W^2 > 4$ GeV^2, $Q^2 > 6$ GeV^2, and $x_{bj} > 0.55$. In neither case are events weighted to reflect the cross section.

Upon propagating the electrons through the CLEO field, one finds a "kink" in the behavior of $1/p$ vs. Δr at the high extreme values of Δr, for GEM pairs including at least one downstream GEM (GEM 4 or 5); see Fig. 1. These events are ones in which the electron has passed near $z = 200$ cm, $r = 150$ cm, where the solenoid iron near the "corner" of the uniform field region gives rise to large (of order 1 T) radial fields, as shown in Figure 2. Steps to mitigate the effects of such radial fields on electrons within our acceptance should be considered. For this report, a v_z dependent cut on Δr was imposed to reject such electrons.

4. Smoothing the field

Before talking about the analysis with the newer field version, a problem that had been present and unexplained in the old analysis needs to be discussed. Because there is no material in the simulation there are no random processes involved, only propagation of charged particles in the field. Figure 3 shows results of a typical fit using the CLEO field as well as a uniform field. For this plot the input data are generated using only a single value of θ_p and z_v. Note the noisy-looking residuals plot for the CLEO field. If there are no random processes, why is the residual not a smooth function of $\Delta\phi$ only?

Zhiwen Zhao recommended changes to some field parameters in GEMC to improve field propagation accuracy, which improved the residuals behavior but still resulted in chaotic-looking fluctuations. The main cause of the problem turned out to be that the field was being modeled using sampled values in fixed size bins of r and z (1 cm by 1 cm); within each bin the field was taken to be constant. As the track momentum was varied, the trajectory would sweep across multiple bin boundaries at which the field changed discontinuously. Modifying GEMC to do a linear interpolation of the field between neighboring bins resulted in smooth behavior and much smaller residuals.

These "noisy" residuals had been seen in the previous work and not understood; they limited the quality of the fits. With the interpolated field, we can model the behavior of the field more precisely. Of course this means demands on our fitting procedure are higher, and contributes to the need for a less simple fit function.

5. Fits for new field

With the present version of the CLEO field and interpolation, the fitting approach used previously fails because $1/(p\Delta\phi)$ varies with respect to $\Delta\phi$. Blindly applying that procedure, even for events from a zero length target with tight cuts on Δr, results in poor fits. Therefore, instead of fitting $1/(p\Delta\phi)$ as a two dimensional function of Δr and R, I fit $1/p$ as a three dimensional function of $\Delta\phi$, Δr, and R.

Specifically, a 3-dimensional histogram of truth values of $1/p$ in the uniform simulation versus $\Delta\phi$, Δr, and R was fit to a 3-dimensional polynomial, denoted $P_3(\Delta\phi, \Delta r, R)$. For

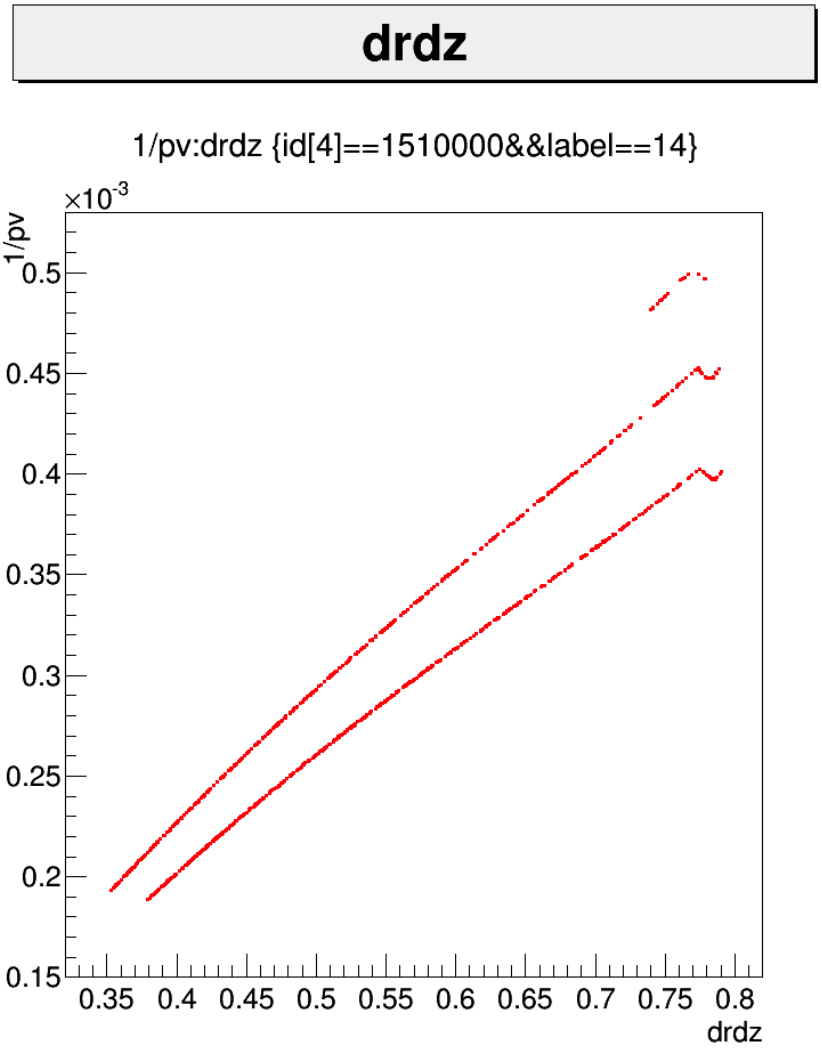

FIGURE 1. $1/p$ vs. Δr for events from a thin target ($z_v = 0$) and for three values of $\Delta\phi$.

good fits I found it necessary for this polynomial to be order 1 in $\Delta\phi$, 4 in Δr, and 3 in R, for a total of 40 floating parameters. In addition, to reduce correlations, these variables were zero shifted by subtracting off average values, adding 3 fixed parameters to the model. Separate fits were done for all 10 possible GEM pairs. Using the resulting functions, any pair of GEM hits corresponding to an electron within our kinematic cuts and outside the "kink" range can be used to reconstruct its momentum to within about 0.01% if at least

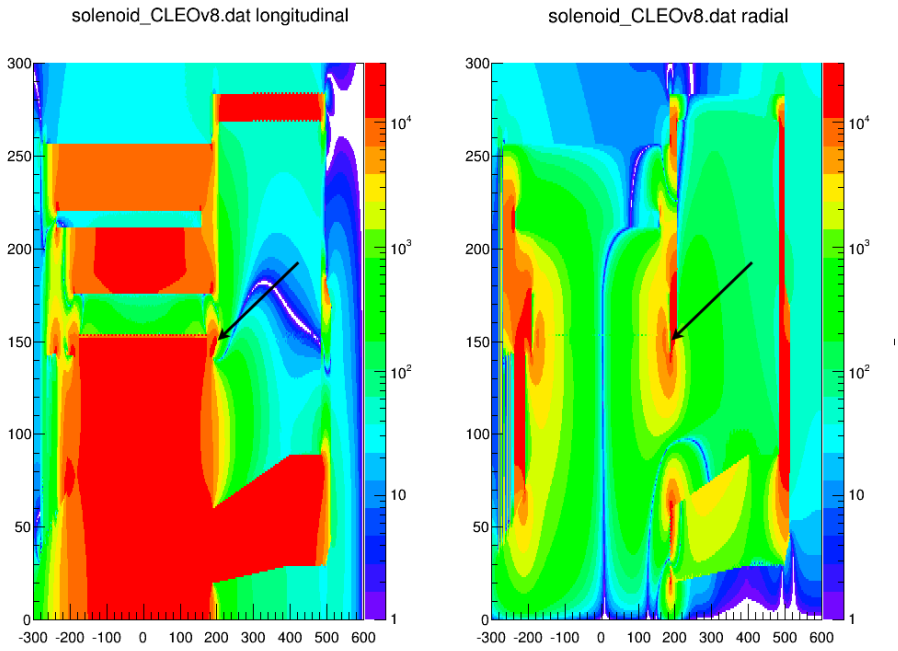

FIGURE 2. Magnitudes of longitudinal (left) and radial (right) components of solenoid_CLEOv8 field, mapped versus z (horizontal axis) and r (vertical axis, both axes in cm). Arrow indicates approximate point through which electrons in the "kink" pass.

one of the GEMs is downstream. For GEMs 1 and 2, 1 and 3, or 2 and 3 the fit residuals are larger, up to about 0.1%.

A similar procedure works to get polynomial functions, $\Theta_3(\Delta\phi, \Delta r, R)$, to estimate θ_p from hit pairs. (I would expect z_v also could be reconstructed but I have not yet done so.)

The functions and their parameters were written to an output ROOT file for use by other scripts.

6. Calbration procedure

These functions were obtained using truth values of the momentum and assuming the field model is accurate. For the experimental calibration, the field model will be only approximately correct, and truth values of the momentum will be unknown. Therefore we need to develop a procedure that works with neither an exact field model nor knowledge of p.

For elastically scattered electrons there is a known relation between p and θ_p, reducing the dimensionality of the problem; if we can measure θ_p we can learn p. In the absence of a field, $\Delta r = \tan\theta_p$. For an approximately longitudinal field, Δr should be only weakly field

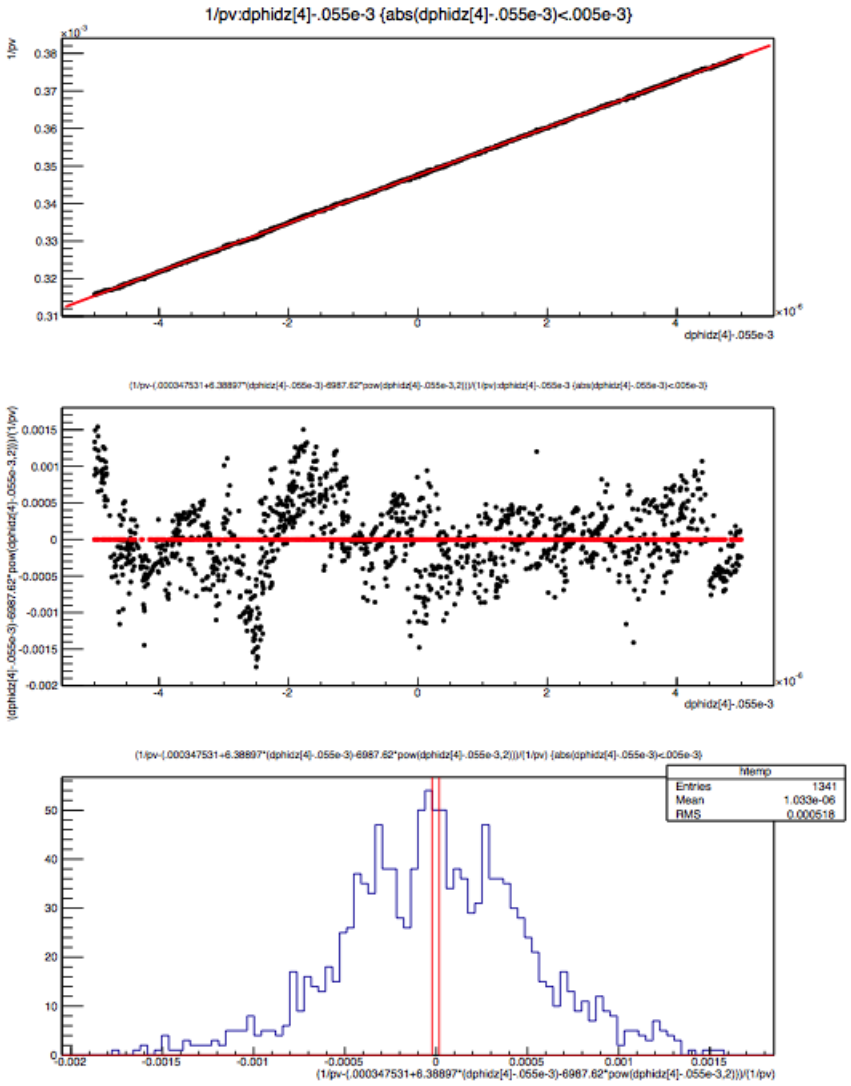

FIGURE 3. Typical plots from analyses of a 1-dimensional problem: (top) $1/p$ vs. $\Delta\phi$ (zero shifted); (middle) relative residual $(1/p_{truth} - 1/p_{fit})/(1/p_{truth})$ vs. $\Delta\phi$; and (bottom) relative residual distribution. Results for CLEO field are shown as black or blue lines or black points; results for a uniform field are shown as red lines or points. Here the field is not interpolated between bins.

dependent. Therefore a 2-dimensional fit of $1/p$ versus Δr and R for Monte Carlo elastics with the CLEO field model may give us a function, $P_2(\Delta r, R)$, to estimate $1/p$ which will work with real elastic data (and the real field) to sufficient accuracy. Then, by using values of this function, we can do a 3-dimensional fit of real elastic data, without knowing the truth value of $1/p$, to obtain our final calibration functions.

In the previous work it seemed this program could be carried out using elastic data at a single energy. However, with the higher order polynomials in use for the current field, elastics at a single energy do not span enough parameter space to get reliable results.

To demonstrate the calibration procedure I did the following:

First, for simulated elastic data at 4.4 GeV with the CLEO field, I obtained 2-dimensional functions $P_2(\Delta r, R)$ (one such function for each GEM pair). Truth values of $1/p$ were used to do the fits. A similar set of functions was found for simulated 6.6 GeV elastics. While θ_p for elastics can be calculated from p, and vice versa, I found it advantageous to do separate fits to get functions $\Theta_2(\Delta r, R)$ to estimate θ_p.

Next, for combined simulated elastic data at 4.4 and 6.6 GeV with a modified field, I obtained 3-dimensional functions $P_3(\Delta\phi, \Delta r, R)$ (one such function for each GEM pair). The modified field I used was 95% of the CLEO field plus 5% of a uniform 1.5 T field; loosely speaking, this is a field in which the radial components are reduced by 5%. Values of $1/p$ obtained from the $P_2(\Delta r, R)$ functions (instead of truth values of $1/p$) were used to do the fits. Similarly, I found 3-dimensional functions $\Theta_3(\Delta\phi, \Delta r, R)$ by fitting values of $\Theta_2(\Delta r, R)$ for elastics at both energies against the three variables.

7. Residuals and biases

Figure 4 shows $1/p$ relative residuals versus p for several elastic cases. On the top left are the residuals, $(1/p - P_2(\Delta r, R))/(1/p)$, for simulated elastics with CLEO field, using GEMs 1 and 4, versus p. The P_2 parameters were obtained from a fit to the same data and truth values for p. Red (green) dots are 4.4 (6.6) GeV elastics. The fit is good at the 10^{-5} level. On the top right are the residuals for the modified field using the same $P_2(\Delta r, R)$ functions. The momentum is biased by a factor of 1 to 7 parts in 10^4.

On the bottom row are similar plots for GEMs 1 and 2. The bias for the modified field is smaller, less than 3 parts in 10^4; presumably this is because the GEMs used are upstream of the largest radial fields.

Figure 5 is a similar set of residuals plots using the $P_3(\Delta\phi, \Delta r, R)$ function; parameters are from a single fit to simulated elastic data at both 4.4 and 6.6 GeV, using the previously obtained $P_2(\Delta r, R)$ function values for p. Data with the CLEO field are on the left and with the modified field on the right. On the top are results using GEMs 1 and 4; on the bottom are GEMs 1 and 2. The fits are worse for the upstream GEMs, but the field dependence is smaller. These plots illustrate how we would calibrate the field experimentally: we would use $P_2(\Delta r, R)$ from a simulation to get estimates of $1/p$ for elastics, which would then be used in a fit of experimental elastic data to to get the $P_3(\Delta\phi, \Delta r, R)$ function parameters. Similar fits were done to get $\Theta_3(\Delta\phi, \Delta r, R)$ for θ_p estimation.

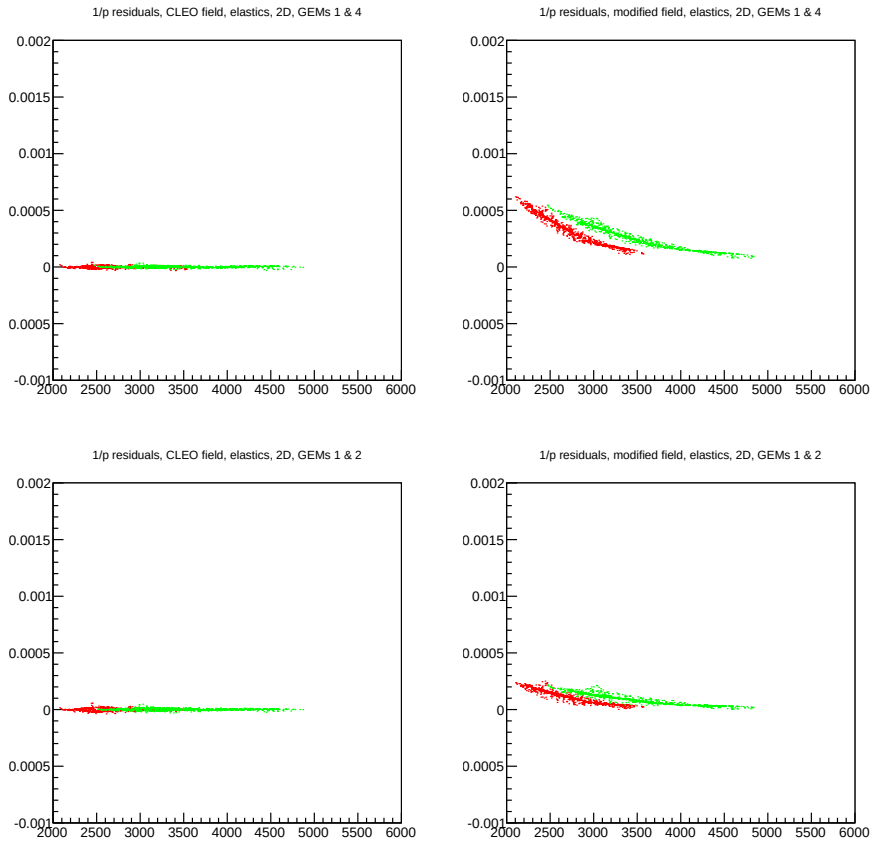

FIGURE 4. Relative residuals for $1/p$ vs. p for elastic data. Red (green) dots are 4.4 (6.6) GeV elastics. Function is $P_2(\Delta r, R)$ with parameters from a fit of true p values in simulations using the CLEO field. Left (right) plots are for CLEO (modified) field; top (bottom) plots use GEMs 1 and 4 (1 and 2).

The 3-dimensional functions thus obtained can be used to extract p and θ_p for uniform data. Figure 6 shows $1/p$ residuals for uniform electrons, and similar plots are seen in Fig. 7 for residuals in θ_p. Given estimates of p and θ_p we can estimate Q^2, and in Figs. 8 and 9 I show residuals for Q^2. For all but the highest momenta, our Q^2 estimate using the upstream GEMs is almost always within 0.05% of the truth value.

8. Detector resolution, multiple scattering, and radiation

To this point I have used truth values for the track positions at the GEMs. Next I want to address the effects of detector resolution. I took the GEM position resolution to

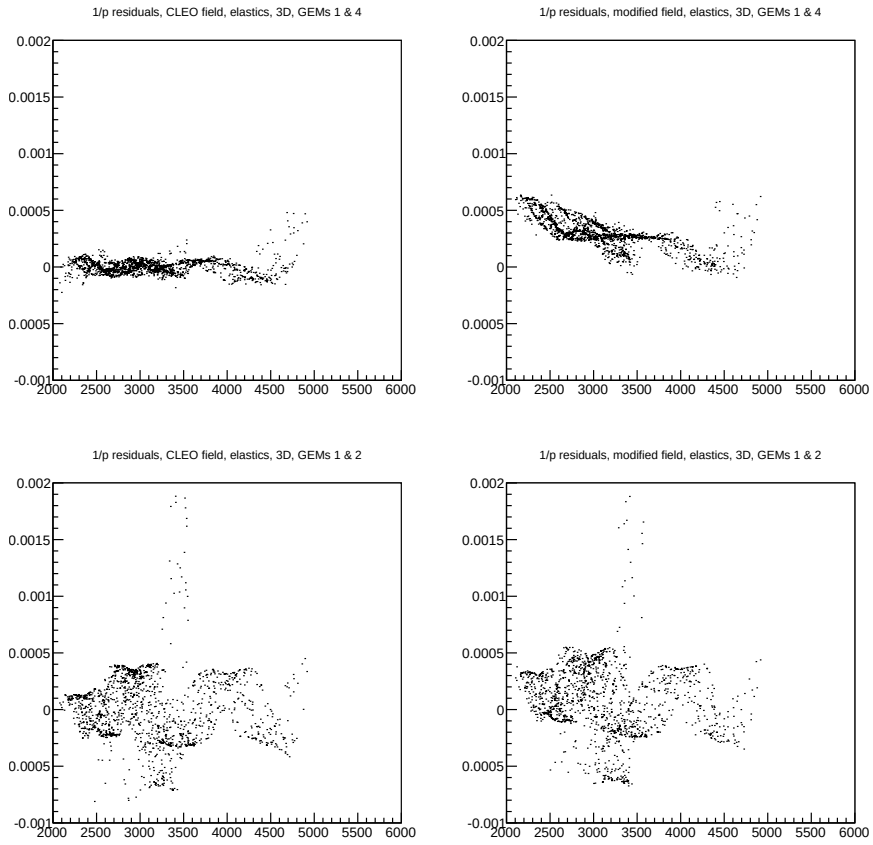

FIGURE 5. Relative residuals for $1/p$ vs. p for elastic data. Function is $P_3(\Delta\phi, \Delta r, R)$ with parameters from a fit of p values from the previously obtained $P_2(\Delta r, R)$ functions. Left (right) plots are for CLEO (modified) field; top (bottom) plots use GEMs 1 and 4 (1 and 2).

be 70 μm[3] for the upstream GEMs, from which I get r resolution $\delta r = 470\mu$m and θ_p resolution $\delta\theta_p = 0.057/r$ mrad (with r in mm). Then I followed the above procedure of first getting P_2 and Θ_2 for the two elastic data sets (with the CLEO field) using the truth values of r and θ_p smeared by Gaussians with these widths; then P_3 and Θ_3 for the combined elastics (again with the CLEO field). Finally I used these functions to get residuals for the uniform data (CLEO field). The resulting p and θ_p resolutions (RMS widths of residuals) are shown in Figs. 10 and 11.

The p fit is poor for $\theta_p \lesssim 22^\circ$, but this is outside our required acceptance. Above that the momentum width is a function of momentum and not θ_p, while the θ_p width is a function of θ_p and not momentum, at least within the kinematics cuts.

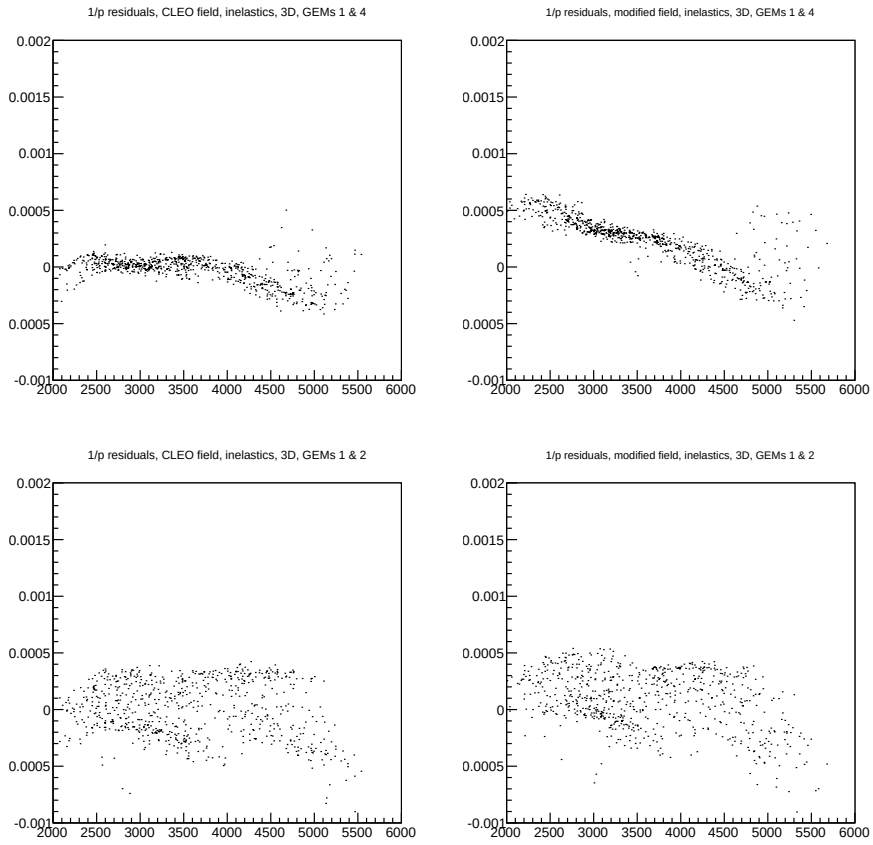

FIGURE 6. Relative residuals for $1/p$ vs. p for uniform data. Function is the previously obtained $P_3(\Delta\phi, \Delta r, R)$. Left (right) plots are for CLEO (modified) field; top (bottom) plots use GEMs 1 and 4 (1 and 2).

Next, I have considered the effects of multiple scattering and radiative processes by analyzing data from simulations that include materials: the LD2 target, detectors, and other apparatus. Extracting the calibration functions P_3 and Θ_3 for such data is problematic; in the absence of additional cuts, the fits are poor and momentum resolutions of several percent are obtained. By contrast, residuals for elastics using P_2 and Θ_2 are not much worse than the no-materials case. The reason can be seen in Fig. 12. On the left is $\Delta r/R$ vs. R for tracks with $p \sim 3$ GeV; the red points are for data without target and detector materials present while the black points are for data with materials. On the right is a similar plot for $\Delta\phi$ vs. R. One can see multiple scattering and radiation distort the distribution of $\Delta\phi$ much more than that of $\Delta r/R$ or R. Since the 2-dimensional fits do not use $\Delta\phi$ while the 3-dimensional fits do, the former are much less affected by the presence of materials than the latter. Note in particular the widely scattered black points in the $\Delta\phi$

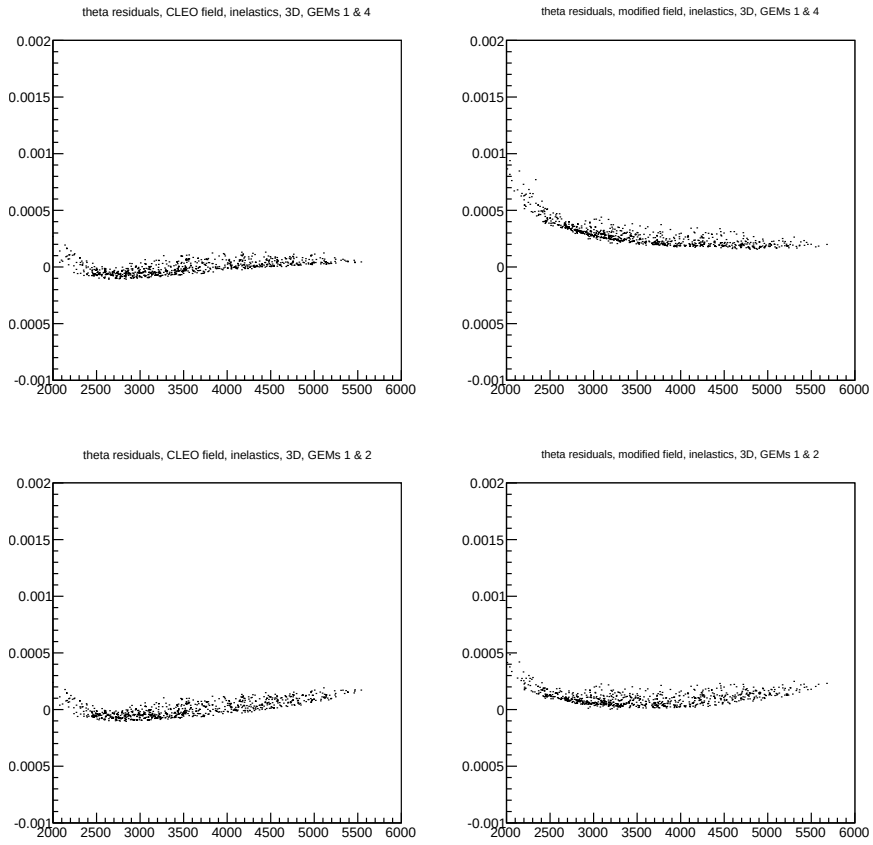

FIGURE 7. Relative residuals for θ_p vs. p for uniform data. Function is $\Theta_3(\Delta\phi, \Delta r, R)$ previously obtained by a fit to elastic data. Left (right) plots are for CLEO (modified) field; top (bottom) plots use GEMs 1 and 4 (1 and 2).

vs. R which lie mainly above, not below, the red points. This asymmetry is presumably due to radiative effects and alters the shapes and mean values, of the $\Delta\phi$ distributions. Such distortions can spoil the calibration function fits and give rise to poor resolutions. It may be possible to recover good calibration functions in an iterative procedure by cutting events that lie in the tails of the momentum distributions.

For the present, to get a handle on resolutions with multiple scattering and radiation, I have simply used the calibration functions obtained without materials (but with detector resolution) to find the residuals for data with materials (and detector resolution). The residual peaks (a sample of 9 momentum residual plots, for various values of p and θ_p, is shown in Fig. 13) are non Gaussian mainly due to the radiative tail on the negative side. A few isolated tail events occur at very large values of the residual, beyond the bounds

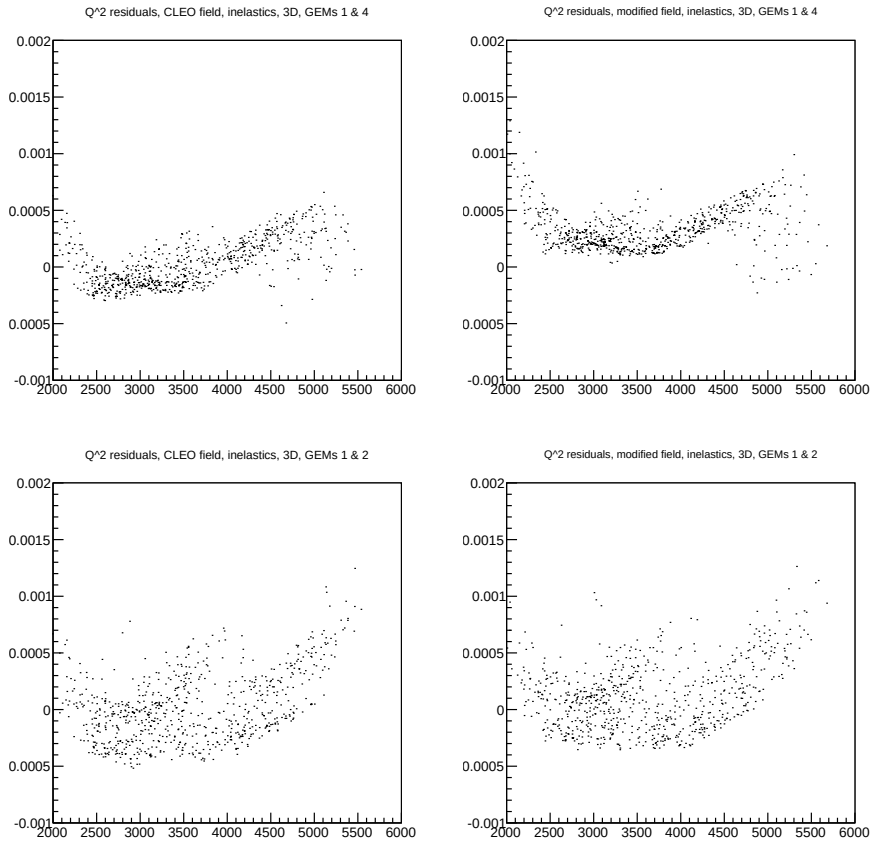

FIGURE 8. Relative residuals for Q^2 vs. p for uniform data, estimated using the previously obtained $P_3(\Delta\phi, \Delta r, R)$ and $\Theta_3(\Delta\phi, \Delta r, R)$ functions. Left (right) plots are for CLEO (modified) field; top (bottom) plots use GEMs 1 and 4 (1 and 2).

shown in the figure. The resolutions shown in Figs. 14 and 15 are widths of Gaussian fits to the peaks. RMS widths, after cutting the largest outliers, are about 60% larger. The momentum resolution varies slowly from about 1% to about 0.9% with increasing momentum and depends weakly on θ_p. The angle resolution is independent of angle, decreasing from about 1.2 mrad to 0.8 mrad with increasing momentum.

9. To be done

Several tasks in this program remain to be done.
In principle it should be possible to extract v_z similarly to p and θ_p.

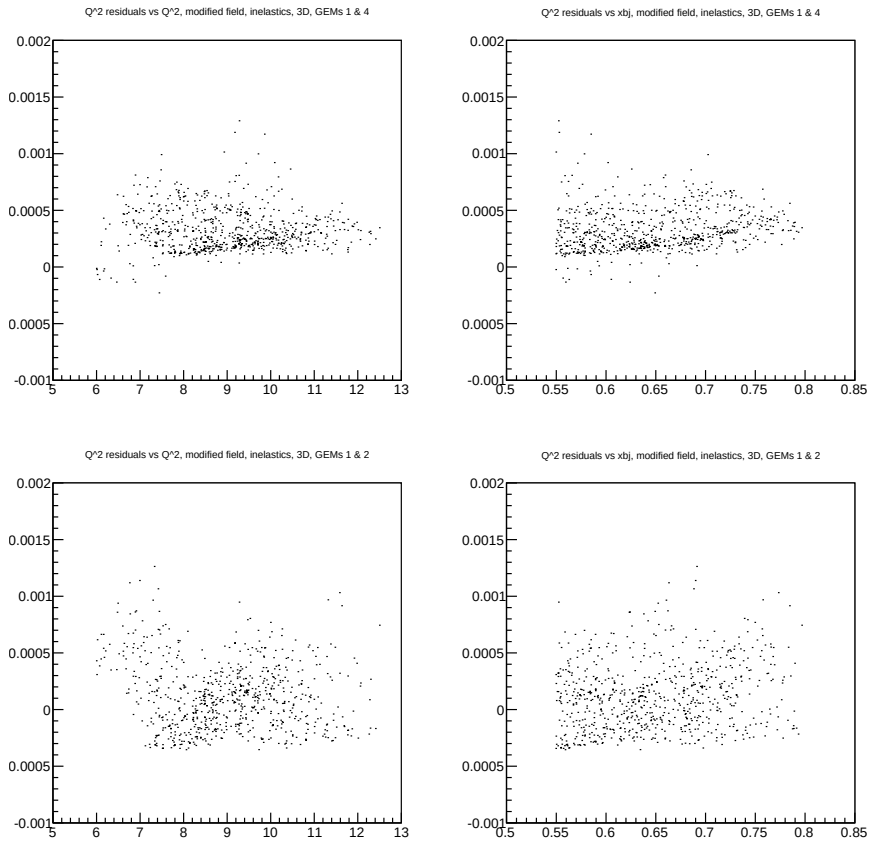

FIGURE 9. Relative residuals for Q^2 vs. Q^2 (left) or vs. x_{bj} (right) for uniform data and modified field, estimated using the previously obtained $P_3(\Delta\phi, \Delta r, R)$ and $\Theta_3(\Delta\phi, \Delta r, R)$ functions. Top (bottom) plots use GEMs 1 and 4 (1 and 2).

The large number of parameters in the calibration functions was driven by quality of fits for the data without detector resolution or materials. In the more realistic data there is enough smearing that lower order polynomials might give equally good fits. This should be explored.

Appropriate cuts, perhaps cuts on tails of momentum distributions applied in an iterative procedure, need to be developed in an effort to get good calibrations from data with multiple scattering and radiative effects.

The "kink region" needs to be dealt with. If the kinks cannot be eliminated with tweaks to the magnet design then we need better ways to handle them in the analysis.

In the simulations used so far, the beam spot size is zero and there is no rastering; consequently $r_v = 0$. More realistic simulations would have finite spot size and rastering.

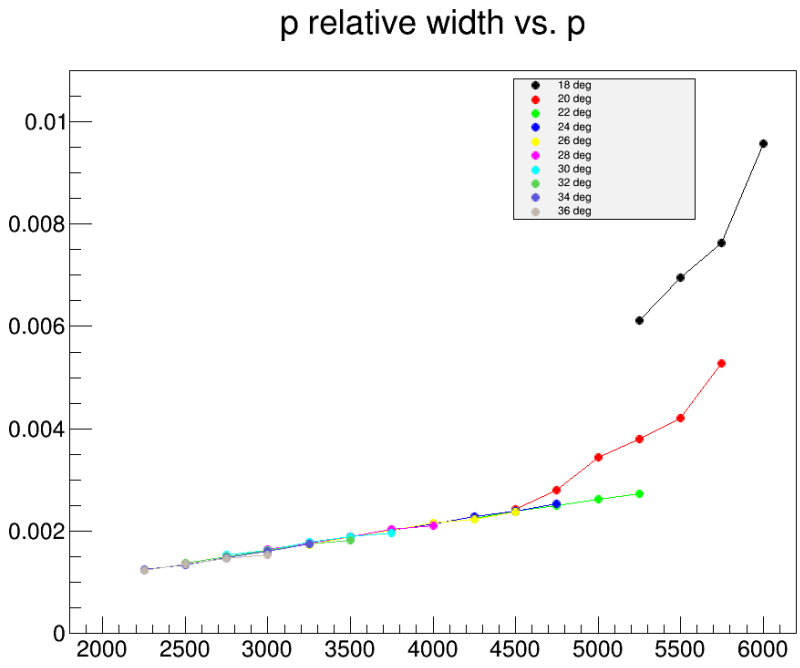

FIGURE 10. Momentum resolution (RMS width of residuals, percent) vs. momentum (MeV) for GEMs 1 and 4 with positions smeared to simulate detector resolution.

Then either the rastered beam's transverse position would need to be subtracted off the hit positions, or the data would have to be binned in transverse position and separate calibrations done for each bin, or both; beam spot size and transverse position resolution would be likely to degrade the resolution for the vertex variables.

REFERENCES

[1] R. Holmes, "Calibration update" (17 Jul 2012).
[2] R. Holmes, "Resolution" (4 Dec 2012).
[3] K. Gnavo, *et al.*, "Large Size GEM for Super Bigbite Spectrometer (SBS) Polarimeter for Hall A 12 GeV program at JLab" (7 Feb 2015) (arXiv:1409.5393v2 [physics.ins-det])

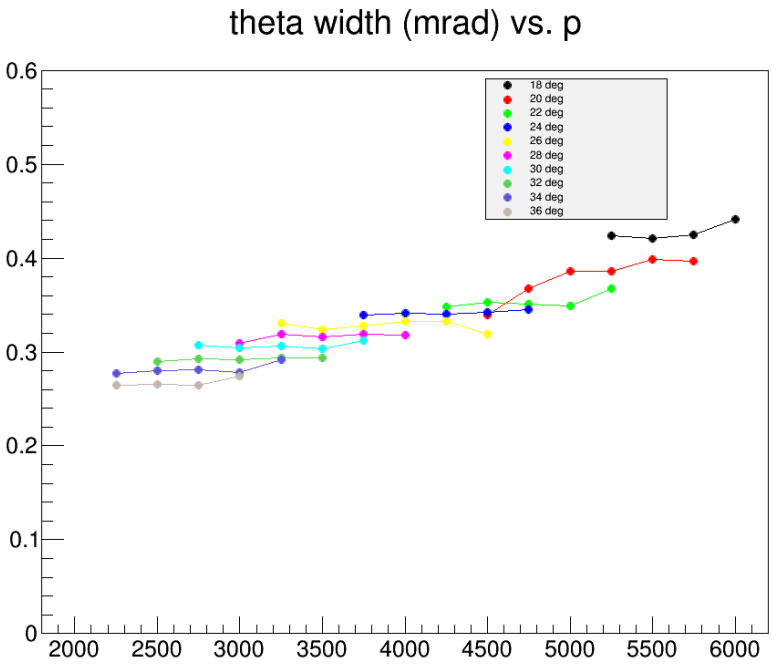

FIGURE 11. Polar angle resolution (RMS width of residuals, mrad) vs. momentum (MeV) for GEMs 1 and 4 with positions smeared to simulate detector resolution.

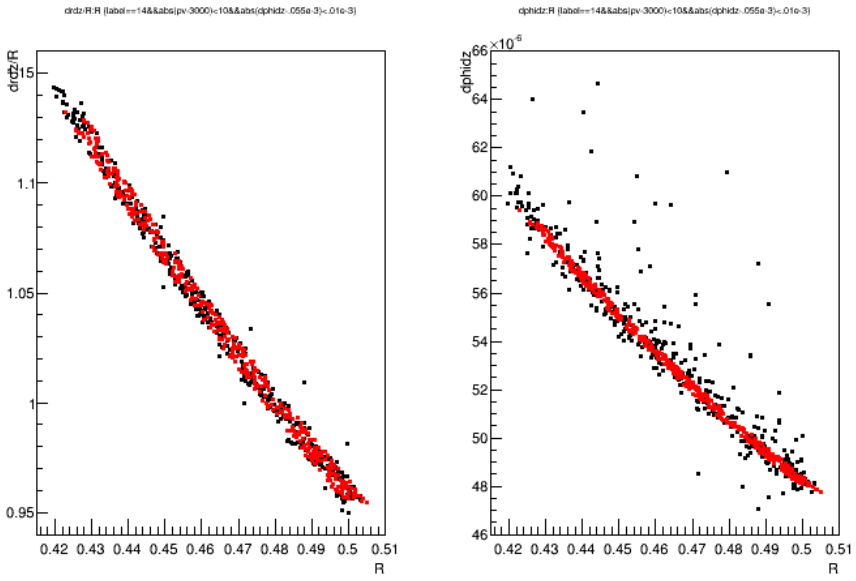

FIGURE 12. $\Delta r/R$ (left) and $\Delta\phi$ (right) vs. R for tracks with $p \sim 3$ GeV, in simulations without (red points) and with (black points) material target and detectors.

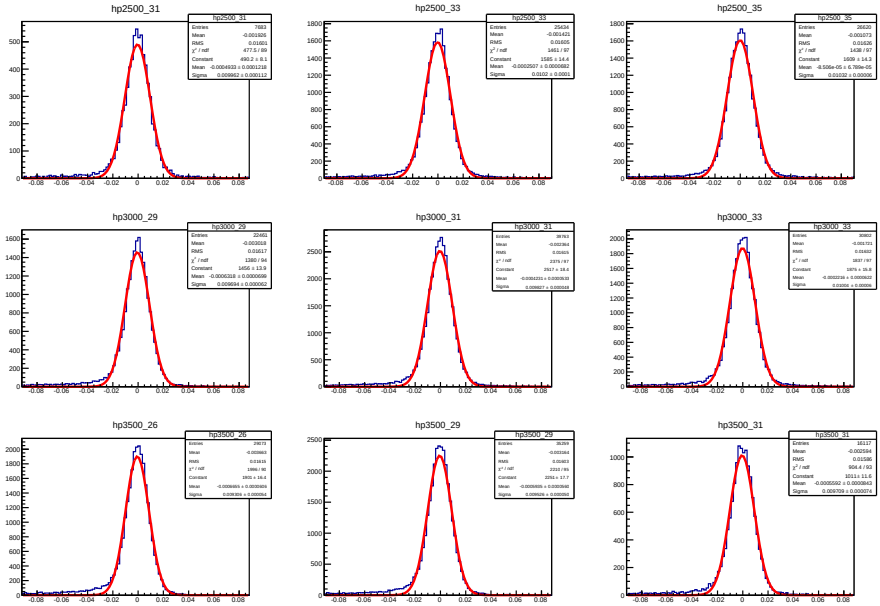

FIGURE 13. Momentum residuals for several values of p and θ_p, showing typical shapes with tails on the negative sides. Red curves are Gaussian fits.

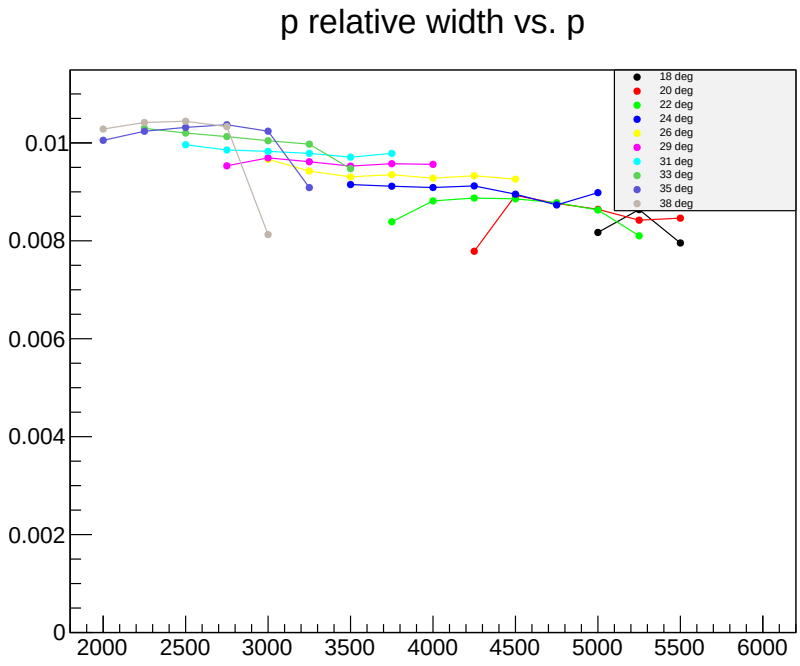

FIGURE 14. Momentum resolution (width of Gaussian fits to residuals, percent) vs. momentum (MeV) for GEMs 1 and 4 with positions smeared to simulate detector resolution. Target and detector materials are included in the data, though the calibration functions come from data without materials.

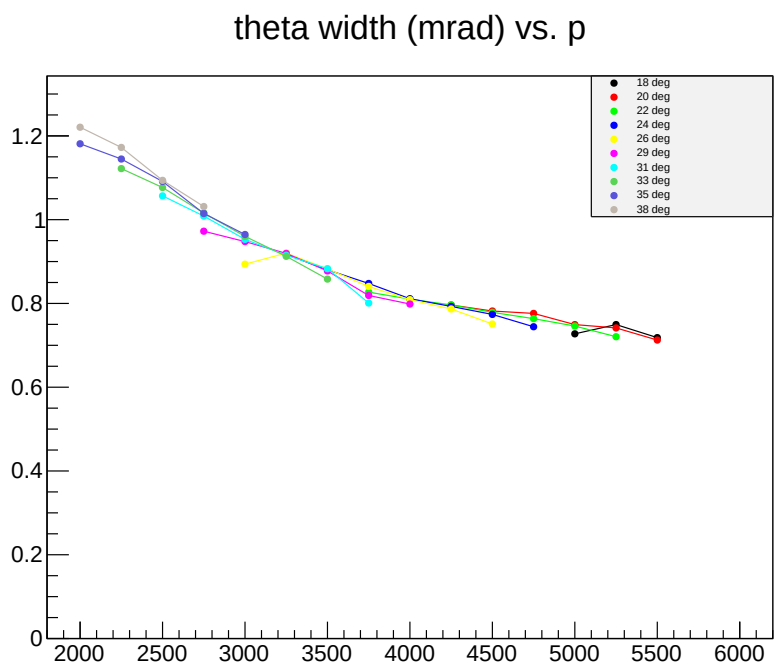

FIGURE 15. Polar angle resolution (width of Gaussian fits to residuals, mrad) vs. momentum (MeV) for GEMs 1 and 4 with positions smeared to simulate detector resolution. Target and detector materials are included in the data, though the calibration functions come from data without materials.